Hindawi Publishing Corporation
International Journal of Photoenergy
Volume 2013, Article ID 247516, 5 pages
http://dx.doi.org/10.1155/2013/247516

Research Article

Green Synthesis of Feather-Shaped MoS_2/CdS Photocatalyst for Effective Hydrogen Production

Yang Liu, Hongtao Yu, Xie Quan, and Shuo Chen

Key Laboratory of Industrial Ecology and Environmental Engineering of Ministry of Education, School of Environmental Science and Technology, Dalian University of Technology, Dalian 116024, China

Correspondence should be addressed to Shuo Chen; shuochen@dlut.edu.cn

Received 31 May 2013; Revised 4 September 2013; Accepted 4 September 2013

Academic Editor: Pierre Pichat

MoS_2/CdS photocatalyst was fabricated by a hydrothermal method for H_2 production under visible light. This method used low toxic thiourea as a sulfur source and was carried out at 200°C. Thus, it was better than the traditional methods, which are based on an annealing process at relatively high temperature (above 400°C) using toxic H_2S as reducing agent. Scanning electron microscopy and transmission electron microscopy images showed that the morphologies of MoS_2/CdS samples were feather shaped and MoS_2 layer was on the surface of CdS. The X-ray photoelectron spectroscopy testified that the sample was composed of stoichiometric MoS_2 and CdS. The UV-vis diffuse reflectance spectra displayed that the loading of MoS_2 can enhance the optical absorption of MoS_2/CdS. The photocatalytic activity of MoS_2/CdS was evaluated by producing hydrogen. The hydrogen production rate on MoS_2/CdS reached 192 μmol·h^{-1}. This performance was stable during three repeated photocatalytic processes.

1. Introduction

Solar hydrogen production from water can provide a clean and renewable energy. It has been considered to be the most promising approach for solving energy and environmental issues at a global level. In this context the fabrication of effective photocatalysts is an important area of research. Many semiconductors such as TiO_2 [1], ZnO [2], Nd_2O_5 [3], and CdS [4] have been reported as useful photocatalysts for hydrogen production. Among these photocatalysts, CdS has received the most attentions, due to its superior light absorption and appropriate conduction-band level [5–8]. However, bare CdS photocatalyst usually suffers from photocorrosion [8, 9], which can be improved by loading a cocatalyst such as noble metal (Pt [4, 10], Au [11], and Rh [12, 13]), WC [14], and WS_2 [15] on the surface of CdS. From the resources and environmental point of view, noble metal and tungsten are limited by their rare availability and high price. Therefore, there is an emerging urge for exploring alternative cocatalysts.

Recently, MoS_2 was reported to be a good cocatalyst, and it has been experimentally confirmed that hydrogen production on CdS with MoS_2 loading is even more efficient than that of CdS with noble metal loading [16–19]. However, for the fabrication of MoS_2/CdS photocatalyst, the poisonous H_2S gas has to be employed as sulfur source, and the calcinations temperature is relatively high (above 400°C [17, 19]). These disadvantages limited the development of this promising photocatalyst. Therefore, it is worthy to find a green method at relatively low temperature with nontoxic sulfur source for the preparation of MoS_2/CdS photocatalyst.

Herein, we developed a hydrothermal method for synthesizing MoS_2/CdS photocatalyst. This method was carried out at only 200°C, and its sulfur source was less toxic thiourea. Their photocatalytic performances were evaluated by producing hydrogen under visible light irradiation.

2. Materials and Methods

2.1. Fabrication of MoS_2/CdS Photocatalyst. According to the pioneer work, thiourea has been chosen as sulfur source to synthesize sulfide [16]. $CdCl_2{\cdot}2H_2O$ and $Na_2MoO_4{\cdot}2H_2O$ worked as precursors of Cd and Mo, respectively. Briefly, $CdCl_2{\cdot}2H_2O$ and thiourea with the molar ratio of 1 : 3 were dissolved in 80 mL deionized water; then various amounts of $Na_2MoO_4{\cdot}2H_2O$ were added into the above solution.

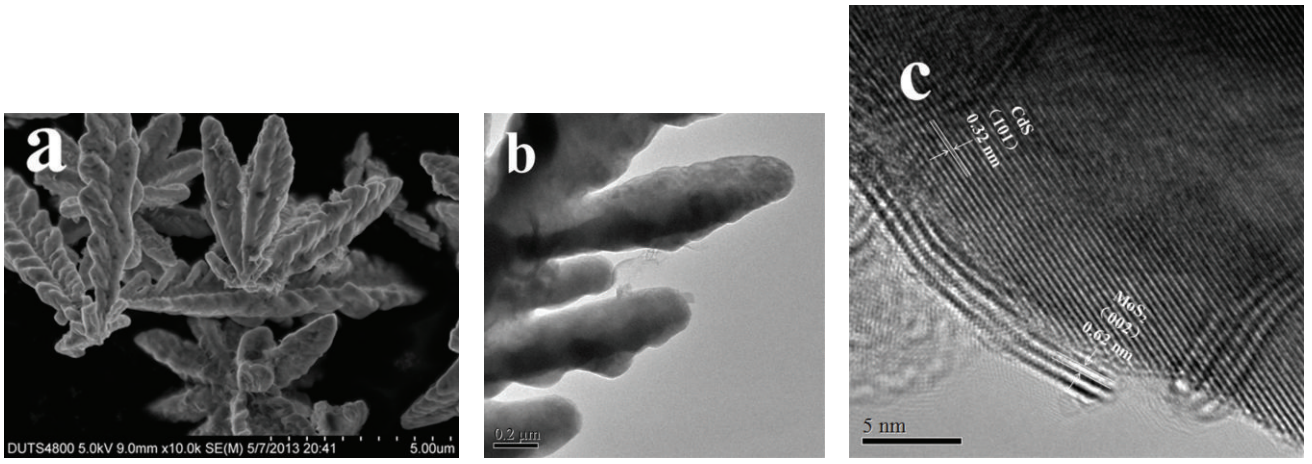

(a) (b) (c)

Figure 1: SEM and TEM images of MoS_2/CdS samples.

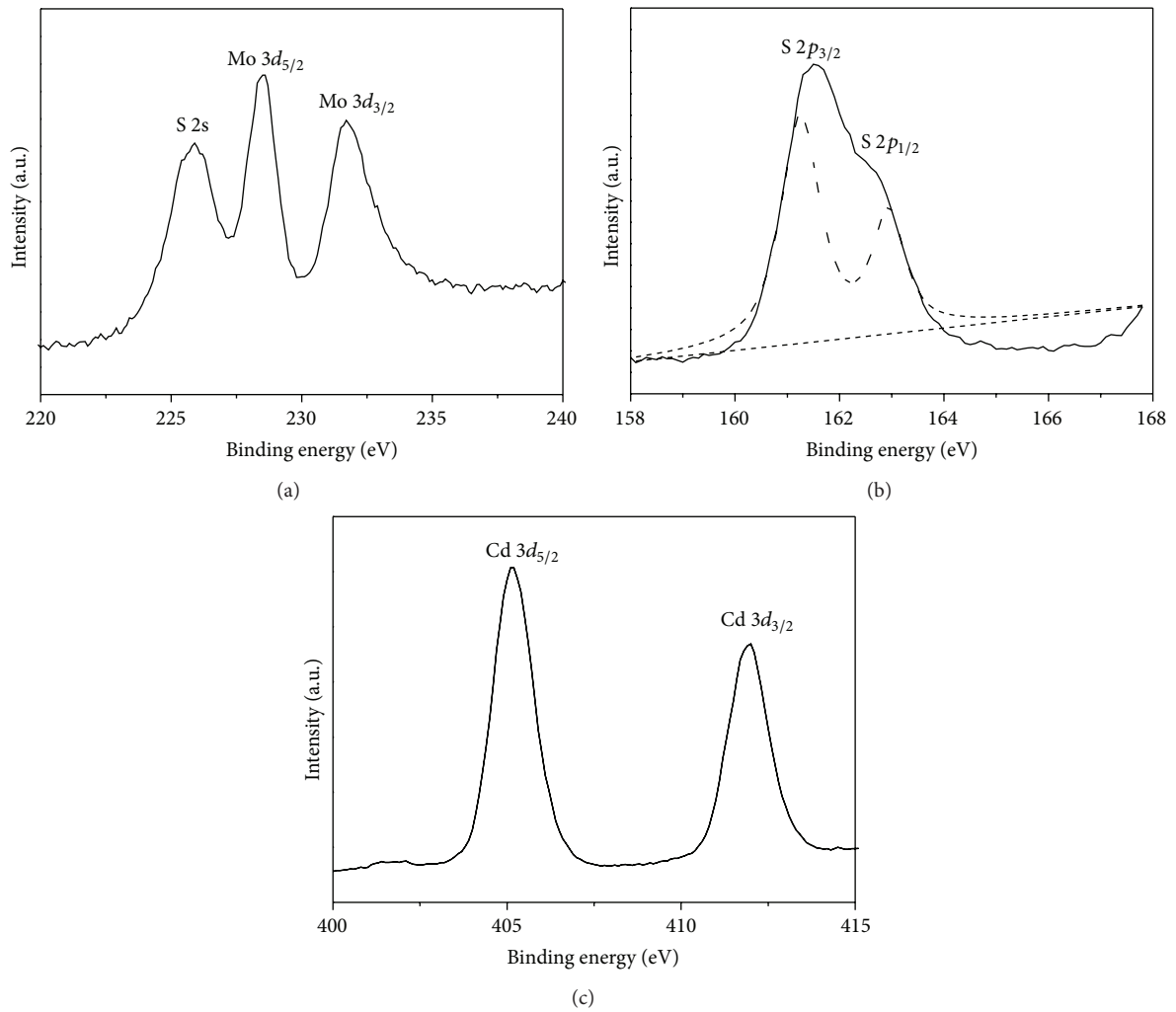

Figure 2: XPS spectra of MoS_2/CdS: (a) Mo 3*d*, (b) S 2*p* and (c) Cd 3*d*.

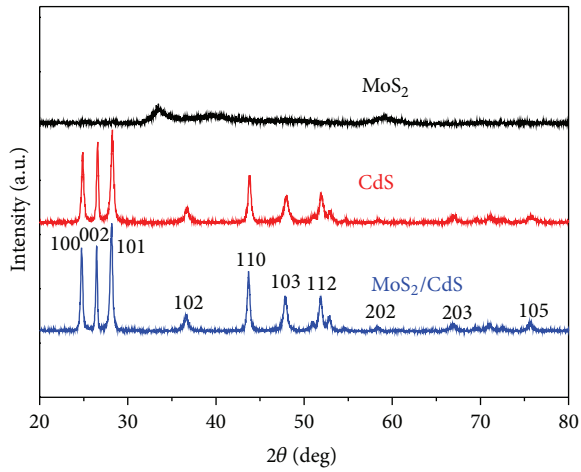

Figure 3: XRD of MoS_2, CdS, and MoS_2/CdS.

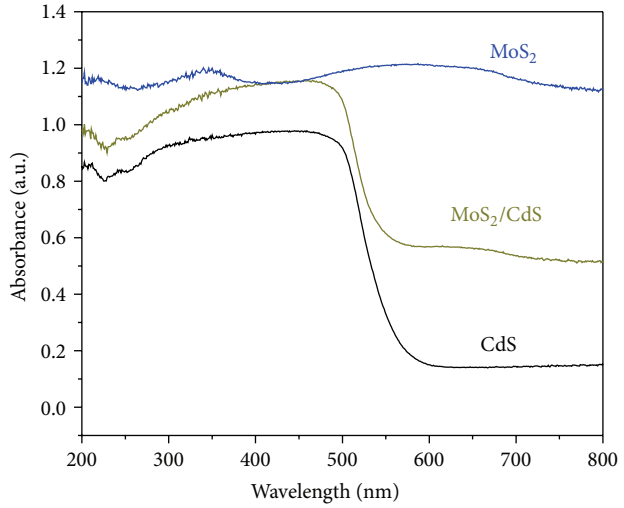

Figure 4: DRS of MoS_2, CdS, and MoS_2/CdS.

The solution was mixed homogeneously in a Teflon-lined stainless steel autoclave (100 mL) followed by sonication for 1 h. Then the Teflon-lined stainless steel autoclave was heated in an air blowing thermostatic oven at 200°C for 24 h. The obtained precipitate was washed with ethanol and water and dried in a vacuum chamber overnight at room temperature.

2.2. Characterization. The morphology of samples was observed by scanning electron microscopy (SEM, Hitachi S-4800) and transmission electron microscopy (TEM, FEI Tecnai G^2 F30). The X-ray photoelectron spectroscopy (XPS) was performed with a VG ESCALAB250 surface analysis system using a monochromatized Al Kα X-ray source (300 W, 20 mA, and 15 kV). The crystal structures of the samples were investigated by an X-ray diffractometer (XRD, Shimadzu LabX XRD-6000) employing Cu Kα radiation accelerating voltage of 40 kV and current of 30 mA over the 2θ range of 20–80°. The optical absorption property of the samples was

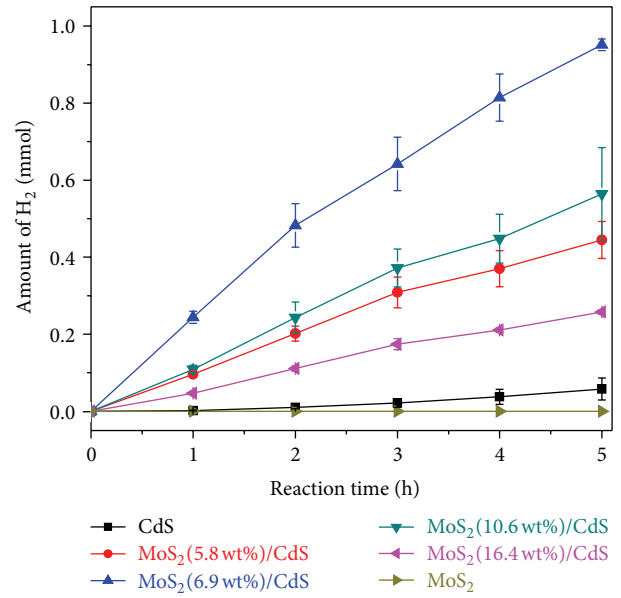

Figure 5: The time courses of photocatalytic H_2 production on MoS_2/CdS with various MoS_2 ratios under visible light irradiation.

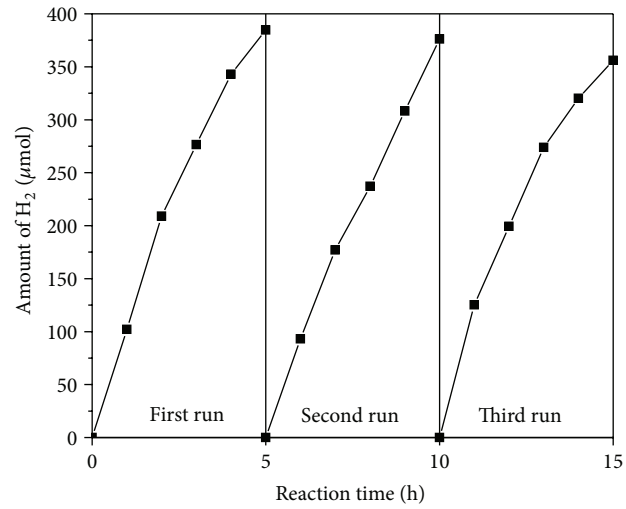

Figure 6: Three consecutive cycling experiments using the same MoS_2 (6.9 wt %)/CdS.

measured by a Shimadzu UV-2450 spectrophotometer with the scanning range from 200 to 800 nm.

2.3. Hydrogen Production Experiments. Hydrogen production experiments were carried out in a Pyrex top-irradiation glass reactor connected to a closed gas-circulation system. The photocatalyst powder (50 mg) was introduced into a 100 mL aqueous solution containing 0.5 M Na_2S and 0.5 M Na_2SO_3 as the sacrificial agent. After stirring, the suspension was irradiated from the top of the reactor by a 300 W Xe lamp with a cut-off filter ($\lambda > 400$ nm). The temperature of reactant solution was maintained constantly at 10°C by a flow of cooling water during the reaction. The H_2 gas was

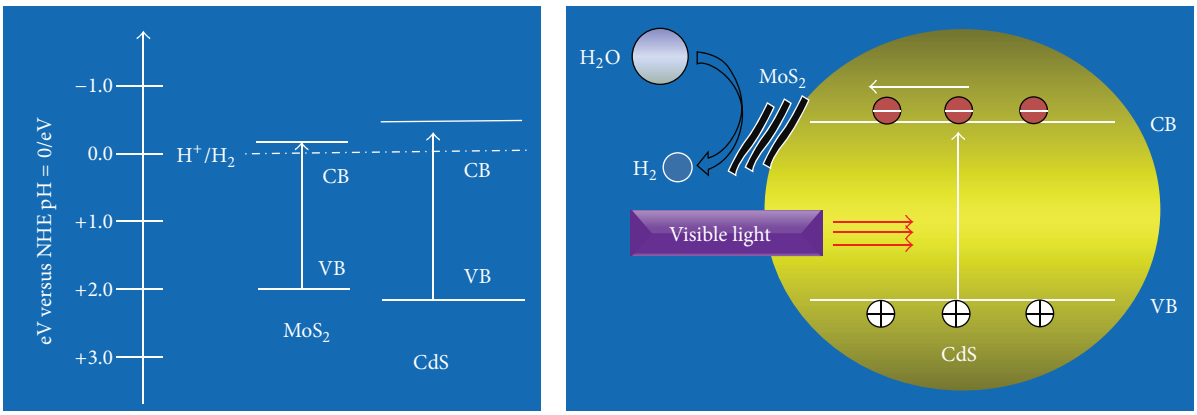

Figure 7: Schematic diagram of H_2 production mechanisms on MoS_2/CdS.

quantified by an online gas chromatograph (Shimadzu, GC-14C, TCD, molecular sieve 5 Å).

3. Results and Discussion

The morphology of the samples was observed by SEM and TEM. The SEM image showed that the samples looked like feather cluster, and the length and width of a feather were about 5 μm and 1 μm, respectively (Figure 1(a)). The TEM image displayed that the feather was composed of fusiform structures (Figure 1(b)). To further magnify, the lattice spacings can be distinguished in Figure 1(c). The magnified HRTEM image in Figure 1(c) exhibits the interlayer spacing of 0.32 nm and 0.62 nm, which correspond to the (101) plane of hexagonal CdS and the (002) plane of hexagonal MoS_2, respectively. It indicated that both MoS_2 and CdS have a good crystallization, and MoS_2 layer was less than 3 nm coated on the surface of CdS.

The chemical composition of samples was investigated by XPS. Figure 2(a) showed the XPS spectrum for Mo 3d. The $3d_{5/2}$ and $3d_{3/2}$ peaks located at 231.7 and 225.9 eV indicated the presence of Mo^{4+} cations. The S 2p spectrum can be found in Figure 2(b). The split peaks of S 2p were at 162.94 and 161.25 eV corresponding to a doublet composed of $3d_{5/2}$ and $3d_{3/2}$. As Figure 2(c) shows, the doublet peaks at 412 and 405.1 eV were ascribed to Cd $3d_{5/2}$ and $3d_{3/2}$. These binding energies are all consistent with the reported values for the MoS_2 and CdS. Together with the results of TEM and XRD, the above results of XPS confirmed that the sample was composed of MoS_2 and CdS.

The crystal structures of MoS_2, CdS, and MoS_2/CdS are investigated by an X-ray diffraction (XRD). As shown in Figure 3, for CdS, the main characteristics peaks correspond, respectively, to the reflection (100), (002), (101), (102), (110), (103), (112), (202), (203), and (105) crystal faces of hexagonal wurtzite structure CdS (JCPDS 41-1049). Compared with MoS_2, no XRD peaks belonging to MoS_2 were detected in MoS_2/CdS, indicating the low amount and fine distribution of MoS_2 on the CdS.

UV-vis diffuse reflectance spectra of MoS_2, CdS, and MoS_2/CdS were shown in Figure 4. It could be seen that the loading of MoS_2 enhanced the light absorption of the MoS_2/CdS composite, which would result in higher light energy utilization.

To observe the effect of MoS_2 ratio to the photocatalytic capability of MoS_2/CdS photocatalysts, MoS_2/CdS samples with various MoS_2 ratios (0 wt%, 5.8 wt%, 6.9 wt%, 10.6 wt%, 16.4 wt%, and 100 wt%) were synthesized, and their respective hydrogen production rates were measured (Figure 5). The hydrogen production rate corresponding to CdS was 11.5 μmol·h^{-1}. The value enhanced obviously, once MoS_2 was coated on the surface of CdS, and reached its maximum on MoS_2 (6.9 wt%)/CdS. Further increase in MoS_2 ratio, the H_2 production rate began to reduce, which could be explained by overloading of MoS_2.

To evaluate the stability of MoS_2 (6.9 wt%)/CdS, three repeated photocatalytic processes were performed. After the third cycle, the H_2 production was 168 μmol·h^{-1}, which reduced only by 7% compared to that of the first one (Figure 6). This insignificant reduction suggested the stability of the MoS_2 (6.9 wt%)/CdS photocatalyst. In other words, the photocorrosion, the inherent drawback of CdS, had been inhibited effectively by loading of MoS_2.

Due to the quantum confinement effect, CB potential of nanoscale MoS_2 has been reported to be about −0.2 eV versus NHE [16], which is sufficiently negative to reduce H^+ to H_2 but more positive than that of CdS (−0.52 eV versus NHE) [20, 21]. Therefore, the photogenerated electrons may transfer from the CB of CdS to the CB of MoS_2 and reduce water to H_2 on the surface of MoS_2. This mechanism agrees with the literature [17, 19] and is shown in Figure 7.

4. Conclusions

A MoS_2/CdS photocatalyst has been successfully synthesized by a green hydrothermal method, which can avoid the disadvantages (such as high energy consumption and toxic sulfur source) of the conventional methods. By controlling the ratio of MoS_2, the H_2 evolution capability of MoS_2/CdS is 17 times greater than that of CdS. It is believed that this green synthesis method can be used to prepare competitive sulfide photocatalysts for efficient solar hydrogen production.

Acknowledgments

The work was supported by the National Basic Research Program of China (2011CB936002). Thanks are due to Shahzad Afzal for the English corrections.

References

[1] A. Fujishima and K. Honda, "Electrochemical photolysis of water at a semiconductor electrode," *Nature*, vol. 238, no. 5358, pp. 37–38, 1972.

[2] M. L. Cubeiro and J. L. G. Fierro, "Selective production of hydrogen by partial oxidation of methanol over ZnO-supported palladium catalysts," *Journal of Catalysis*, vol. 179, no. 1, pp. 150–162, 1998.

[3] X. Chen, T. Yu, X. Fan et al., "Enhanced activity of mesoporous Nb_2O_5 for photocatalytic hydrogen production," *Applied Surface Science*, vol. 253, no. 20, pp. 8500–8506, 2007.

[4] M. Matsumura, Y. Saho, and H. Tsubomura, "Photocatalytic hydrogen production from solutions of sulfite using platinized cadmium sulfide powder," *Journal of Physical Chemistry*, vol. 87, no. 20, pp. 3807–3808, 1983.

[5] D. W. Jing and L. J. Guo, "A novel method for the preparation of a highly stable and active CdS photocatalyst with a special surface nanostructure," *Journal of Physical Chemistry B*, vol. 110, no. 23, pp. 11139–11145, 2006.

[6] J. S. Jang, U. A. Joshi, and J. S. Lee, "Solvothermal synthesis of CdS nanowires for photocatalytic hydrogen and electricity production," *Journal of Physical Chemistry C*, vol. 111, no. 35, pp. 13280–13287, 2007.

[7] N. Z. Bao, L. M. Shen, T. Takata, and K. Domen, "Self-templated synthesis of nanoporous CdS nanostructures for highly efficient photocatalytic hydrogen production under visible light," *Chemistry of Materials*, vol. 20, no. 1, pp. 110–117, 2008.

[8] D. Meissner, R. Memming, and B. Kastening, "Photoelectrochemistry of cadmium sulfide. 1. Reanalysis of photocorrosion and flat-band potential," *Journal of Physical Chemistry*, vol. 92, no. 12, pp. 3476–3483, 1988.

[9] Y. B. Chen, L. Z. Wang, G. Q. Lu, X. Yao, and L. Guo, "Nanoparticles enwrapped with nanotubes: a unique architecture of CdS/titanate nanotubes for efficient photocatalytic hydrogen production from water," *Journal of Materials Chemistry*, vol. 21, no. 13, pp. 5134–5141, 2011.

[10] M. Matsumura, S. Furukawa, Y. Saho, and H. Tsubomura, "Cadmium sulfide photocatalyzed hydrogen production from aqueous solutions of sulfite: effect of crystal structure and preparation method of the catalyst," *Journal of Physical Chemistry*, vol. 89, no. 8, pp. 1327–1329, 1985.

[11] T. T. Yang, W. T. Chen, Y. J. Hsu, K. H. Wei, T. Y. Lin, and T. W. Lin, "Interfacial charge carrier dynamics in core-shell Au-CdS nanocrystals," *Journal of Physical Chemistry C*, vol. 114, no. 26, pp. 11414–11420, 2010.

[12] Y. M. Tricot and J. H. Fendler, "Visible light induced hydrogen production from in situ generated colloidal rhodium-coated cadmium sulfide in surfactant vesicles," *The Journal of the American Chemical Society*, vol. 106, no. 8, pp. 2475–2476, 1984.

[13] Y. M. Tricot and J. H. Fendler, "Colloidal catalyst-coated semiconductors in surfactant vesicles: in situ generation of Rh-coated CdS particles in dihexadecylphosphate vesicles and their utilization for photosensitized charge separation and hydrogen generation," *The Journal of the American Chemical Society*, vol. 106, no. 24, pp. 7359–7366, 1984.

[14] A. T. Garcia-Esparza, D. Cha, Y. Ou, J. Kubota, K. Domen, and K. Takanabe, "Tungsten carbide nanoparticles as efficient cocatalysts for photocatalytic overall water splitting," *ChemSusChem*, vol. 6, no. 1, pp. 168–181, 2013.

[15] D. W. Jing and L. J. Guo, "WS_2 sensitized mesoporous TiO_2 for efficient photocatalytic hydrogen production from water under visible light irradiation," *Catalysis Communications*, vol. 8, no. 5, pp. 795–799, 2007.

[16] Q. Xiang, J. Yu, and M. Jaroniec, "Synergetic effect of MoS_2 and graphene as cocatalysts for enhanced photocatalytic H_2 production activity of TiO_2 nanoparticles," *The Journal of the American Chemical Society*, vol. 134, no. 15, pp. 6575–6578, 2012.

[17] G. Chen, D. Li, F. Li et al., "Ball-milling combined calcination synthesis of MoS_2/CdS photocatalysts for high photocatalytic H_2 evolution activity under visible light irradiation," *Applied Catalysis A*, vol. 443-444, pp. 138–144, 2012.

[18] Y. G. Li, H. L. Wang, L. M. Xie, Y. Liang, G. Hong, and H. Dai, "MoS_2 nanoparticles grown on graphene: an advanced catalyst for the hydrogen evolution reaction," *The Journal of the American Chemical Society*, vol. 133, no. 19, pp. 7296–7299, 2011.

[19] X. Zong, H. Yan, G. Wu et al., "Enhancement of photocatalytic H_2 evolution on CdS by loading MoS_2 as cocatalyst under visible light irradiation," *Journal of the American Chemical Society*, vol. 130, no. 23, pp. 7176–7177, 2008.

[20] J. P. Wilcoxon, P. P. Newcomer, and G. A. Samara, "Synthesis and optical properties of MoS_2 and isomorphous nanoclusters in the quantum confinement regime," *Journal of Applied Physics*, vol. 81, no. 12, pp. 7934–7944, 1997.

[21] W. Ho, J. C. Yu, J. Lin, J. Yu, and P. Li, "Preparation and photocatalytic behavior of MoS_2 and WS_2 nanocluster sensitized TiO_2," *Langmuir*, vol. 20, no. 14, pp. 5865–5869, 2004.